

# Decoding the bispectrum of single-field inflation

Raquel H. Ribeiro,<sup>a</sup> David Seery<sup>b</sup>

<sup>a</sup>Department of Applied Mathematics and Theoretical Physics  
Centre for Mathematical Sciences, Wilberforce Road  
Cambridge CB3 0WA, United Kingdom

<sup>b</sup>Astronomy Centre, University of Sussex  
Falmer, Brighton BN1 9QH, United Kingdom

E-mail: [R.Ribeiro@damtp.cam.ac.uk](mailto:R.Ribeiro@damtp.cam.ac.uk), [D.Seery@sussex.ac.uk](mailto:D.Seery@sussex.ac.uk)

**Abstract.** Galileon fields arise naturally from the decoupling limit of massive gravities, and possess special self-interactions which are protected by a spacetime generalization of Galilean symmetry. We briefly revisit the inflationary phenomenology of Galileon theories. Working from recent computations of the fluctuation Lagrangian to cubic order in the most general model with second-order equations of motion, we show that a distinct shape is present but with suppressed amplitude. A similar shape has been found in other higher-derivative models. It may be visible in a theory tuned to suppress the leading-order shapes, or if the overall bispectrum has large amplitude. Using a partial-wave expansion of the bispectrum, we suggest a possible origin for the frequent appearance of this shape. It follows that models with very disparate microphysics can produce very similar bispectra. We argue that it may be more profitable to distinguish these models by searching for relations between the amplitudes of these common shapes. We illustrate this method using the examples of DBI and  $k$ -inflation.

**Keywords:** inflation, cosmology of the very early universe, cosmological perturbation theory, non-gaussianity

# 1 Introduction

Over the last few decades, advances in observational cosmology have led to a detailed picture of the microwave sky [1–3], now known to be almost smooth with fluctuations at the level of 1 part in  $10^5$ . Among the most popular proposals for the mechanism which seeded these small perturbations is inflation, in which the universe underwent a quasi-de Sitter expansion [4, 5]. When combined with quantum mechanics, inflation allows the growth of density fluctuations which classicalize after horizon crossing [6]. They are subsequently imprinted in the CMB as temperature anisotropies. The statistics of the observable temperature field map directly from the primordial density perturbation, which in turn depends on the microphysics governing the very early universe.

The link with microscopic physics suggests that it may be possible to distinguish different models giving rise to inflation by studying three- and higher  $n$ -point correlations [7]. Current observations suggest that departures from gaussianity are small, but non-gaussian correlations are generated at a low level by most microscopic models and it remains worthwhile to search for them. Computationally and observationally the best place to look is the bispectrum, which contains multiple sources of information: a number of distinct shapes [8] or “channels”—analogous to, but more complicated than, the Mandelstam channels of  $2 \rightarrow 2'$  scattering—together with their amplitudes. The shapes depend on the three-body interactions responsible for generating nontrivial correlations, and the amplitudes measure their relative importance. For reviews, see Refs. [9, 10]. Recent work employing the bispectrum as a discriminant of microphysics includes Refs. [11–17].

If gravity is modified in the infrared, perhaps in a way which accounts for our presently accelerating phase, then this may leave traces in the primordial density fluctuation [18, 19]. Recently there has been interest in “Galileon” fields, which can be thought of as an effective *short*-distance description of longitudinal graviton modes near the decoupling limit of massive gravity [20–22], where  $M_{\text{P}} \rightarrow \infty$  while the cutoff remains fixed. A clear discussion is given in the review by Hinterbichler [23].

A Galileon singlet owes its name to invariance under the transformation

$$\phi(x) \rightarrow \phi(x) + b_\mu x^\mu + c, \tag{1.1}$$

for constant  $b_\mu$  and  $c$ . Eq. (1.1) is a spacetime version of a Galilean transformation, first noticed in the DGP model [24, 25]. It incorporates the shift symmetry  $\phi \rightarrow \phi + c$ , which implies that  $\phi$  can support a long-lived inflationary epoch in the early universe. Indeed, in this scenario the principal difficulty is *ending* inflation. To do so one must stabilize the field, typically by introducing a potential. Because this breaks (1.1) by design, further Galilean-violating terms may be generated radiatively. It may then be technically unnatural to start from an action which approximately respects (1.1).

In Ref. [11] it was argued that this difficulty can be avoided. Taking the potential to be sufficiently mild, Galilean-violating radiative corrections are suppressed, making

a Lagrangian dominated by terms respecting (1.1) technically natural. The prospects for inflation have been studied by several authors, often relaxing invariance under (1.1) and requiring only the weaker condition of second-order equations of motion [14, 26–30]. The most general action of this type was written down over thirty-five years ago by Horndeski [31], and later revisited by several authors [30, 32–34]. The first bispectrum estimate was obtained by Mizuno & Koyama [27], who worked with a model where the most relevant Lagrangian operator was  $(\partial\phi)^2\Box\phi$ . The result for the complete covariant Galileon, in the decoupling limit, was given in Ref. [11]. A class of related models was considered by Creminelli et al. [13]. More recently, Gao & Steer [14] (see also Renaux-Petel [16]) and de Felice & Tsujikawa [15] obtained the bispectrum for the entire Horndeski action and retained the coupling to gravity.

In simple models, the bispectrum is practically determined by Lorentz invariance of the underlying Lagrangian and the unbroken spatial symmetries of de Sitter space [35]. In Galileon models some of this simplicity is lost, and the bispectrum can be more complicated. Nevertheless, Creminelli et al. were able to conclude that no Lagrangian operators became available beyond those which could already be realized in simpler models [13]. Therefore the distinctiveness of the Galileon bispectrum lies only in their relative amplitudes. In practice this means that the models could be difficult to distinguish. The recent analyses of Refs. [14–16] have extended this disappointing conclusion to the full Horndeski action.

Although no new operators are present, the number of linearly independent *shapes* depends on the number of arbitrarily adjustable coefficients in the Lagrangian. In this paper we revisit the question of how many shapes should be expected. At leading order, we find one extra channel typically becomes available—although with suppressed amplitude—which is similar to the shape identified by Creminelli et al. [13] and rediscovered at next-order in  $P(X, \phi)$  models in Ref. [36].<sup>1</sup> This apparent universality is surprising; although the action used by Creminelli et al. is “Galileon,” it is not closely related to that of Refs. [11, 36]. Therefore the similarity of their bispectra could not easily have been anticipated: they are intricate objects having no simple connexion to each other. We employ a partial-wave expansion of the bispectrum to explain some features of this shape. We find that the basis suggested by Fergusson et al. [37] is useful in describing the primordial bispectrum, and gives guidance concerning the distinguishable shapes which can be expected. We give a brief sketch of how a decomposition into these partial waves can be used to derive “consistency equations,” which express predictions of the theory as relations between observable quantities. By determining whether these relations are satisfied, it is possible to rule out classes of scenarios.

---

<sup>1</sup>It was remarked in Ref. [36] that these shapes are visually quite similar. They have a relatively strong cosine [8], typically of order  $\sim 0.9$ . However, there are differences which we will discuss in §3.

*Outline.*—This paper is organized as follows. In §2 we briefly review Galileon inflation and explore the bispectrum shapes at leading order in slow-roll. We show there is an orthogonal shape with suppressed amplitude, which turns out to be related to one present in other single-field models. To understand the recurrence of this shape, in §3 we apply a decomposition of bispectrum shapes in terms of an orthogonal basis. We argue that it may be possible to derive model independent tests using the coefficients of these linear decompositions as appropriate observables. We conclude in §4.

We work in units where  $\hbar = c = 1$ , and define the reduced Planck mass to be  $M_{\text{P}} = (8\pi G)^{-1/2}$ , where  $G$  is Newton’s gravitational constant. When discussing the common bispectrum templates, we denote them “equilateral,” “orthogonal,” “enfolded,” and “local” to distinguish the orthogonal template and other shapes which may or may not be orthogonal to each other.

## 2 Shapes in single-field inflation

**Background.** Beyond the DGP model, the first Galileon theories were constructed by Nicolis et al. [38], who restricted their discussion to a Minkowski background. Their theory was designed to produce second-order equations of motion, even though the action included high-order combinations of derivatives. Higher-order equations of motion would have implied propagating ghosts, and a loss of unitarity when interpreted as a quantum theory. The success of Nicolis et al. in achieving second-order equations of motion was later understood from a more general point of view [39].

For application to the early universe, the Galileon must be promoted to curved spacetime. To protect the important property of second-order equations of motion, one must introduce non-minimal couplings to the curvature. The result is the “covariant” theory of Deffayet et al. [40]. Later work on curved backgrounds includes Refs. [34, 41–44]. We write the Galileon field  $\phi$ . On a de Sitter background, where  $a(t) = \exp(Ht)$ , it is spatially homogeneous and depends only on time,  $t$ . The action is

$$S = \int d^4x a^3 \left\{ \frac{c_2}{2} \dot{\phi}^2 + \frac{2c_3 H}{\Lambda^3} \dot{\phi}^3 + \frac{9c_4 H^2}{2\Lambda^6} \dot{\phi}^4 + \frac{6c_5 H^3}{\Lambda^9} \dot{\phi}^5 - V(\phi) \right\}. \quad (2.1)$$

The potential  $V(\phi)$  is chosen to softly break the Galilean invariance and is necessary to end inflation, as discussed in §1. The scale  $\Lambda$  is the naïve cutoff of the theory. In practice, a Vainshtein effect can allow (2.1) to describe fluctuations at higher energies [45]. The most general models allow the  $c_i$  to be unconstrained, unless one demands compatibility with late-time cosmological or laboratory tests [46–49]. This is optional because it need not be supposed that  $\phi$  is active in the post-inflationary universe. If the Galileon field was present only during inflation, then constraints on  $c_i$  follow by demanding agreement with the standard inflationary observables. Where the Galileon theory arises from the decoupling limit of a ghost-free massive gravity, other constraints may arise [20].

**Fluctuations.** We briefly review the calculation of inflationary perturbations. The Horndeski action is sufficiently general to include the covariant Galileon together with other theories which do not exhibit Galilean symmetry [26, 28, 30, 34, 50]. It turns out to be no more complicated to give the analysis for the Horndeski action, which we do for the sake of generality. Including gravitational effects, three-body interactions among scalar fluctuations in Horndeski’s model are described by the action [14–16]

$$S \supseteq \int d^3x d\tau \left\{ a^2 M^2 [\zeta'^2 - c_s^2 (\partial\zeta)^2] + a\Lambda_1 \zeta'^3 + a^2 \Lambda_2 \zeta \zeta'^2 + a^2 \Lambda_3 \zeta (\partial\zeta)^2 + a^2 \Lambda_4 \zeta' \partial_i \zeta \partial^i (\partial^{-2} \zeta') + a^2 \Lambda_5 \partial^2 \zeta (\partial_i \partial^{-2} \zeta')^2 \right\}. \quad (2.2)$$

In writing this action we have exploited our freedom to integrate by parts, and removed redundant couplings using the equations of motion. Primed quantities are differentiated with respect to conformal time,  $\tau = \int_{\infty}^t dt/a(t)$ . The field  $\zeta$  is the primordial curvature perturbation, and is related to the field fluctuation at linear order by the usual rule  $\zeta = H\delta\phi/\dot{\phi}$ . Its fluctuations propagate at the phase velocity  $c_s$ . The mass  $M$  sets the scale of the action. Specializing to the covariant Galileon would correspond to specific assignments of the  $\Lambda_i$ , but the detailed form of these coefficients will not be important for our discussion. For Horndeski’s general action the  $\Lambda_i$  can be adjusted independently.

## 2.1 Shapes

**Inner product.** Conservation of 3-momentum in the bispectrum requires that the momenta  $\mathbf{k}_i$  generate a triangle in momentum space. The bispectrum is a function on this space of triangles. Babich et al. [8] described its functional form as the “shape” of the bispectrum and introduced a measure to distinguish qualitatively different shapes. Define an inner product between two bispectra  $B_1, B_2$  by the rule

$$\langle B_1, B_2 \rangle \equiv \int_{\text{triangles}} dk_1 dk_2 dk_3 S_1(k_1, k_2, k_3) S_2(k_1, k_2, k_3), \quad (2.3)$$

where  $B_i = (k_1 k_2 k_3)^{-2} S_i$ , and  $S_i$  is called the *shape*. The norm of any bispectrum is  $\|B\| = \langle B, B \rangle^{1/2}$ , and the cosine between two bispectra is the normalized inner product,  $\cos(B_1, B_2) \equiv \langle B_1, B_2 \rangle / \|B_1\| \|B_2\|$ . Further details can be obtained from Refs. [8, 37, 51]. Our conventions, particularly for assigning meaning to divergences in the squeezed limit, follow Ref. [36].

The bispectrum,  $B$ , is defined to satisfy

$$\langle \zeta(\mathbf{k}_1) \zeta(\mathbf{k}_2) \zeta(\mathbf{k}_3) \rangle = (2\pi)^3 \delta(\mathbf{k}_1 + \mathbf{k}_2 + \mathbf{k}_3) B(k_1, k_2, k_3). \quad (2.4)$$

For a general Horndeski model,  $B$  will receive contributions at leading order from all operators in (2.2). This yields  $B = (k_1 k_2 k_3)^{-2} \sum_a S_a$ , where each operator yields a

shape  $S_a$ , and  $a$  labels the distinct operators in the Lagrangian. We plot the  $S_a$  in table 1, computed at leading order in the slow-roll approximation, and quote their cosines with the common templates of CMB analysis in table 2. The  $\zeta'^3$ ,  $\zeta'\partial\zeta\partial\partial^{-2}\zeta'$  and  $\partial^2\zeta(\partial\partial^{-2}\zeta')^2$  shapes are highly correlated with the **equilateral** template. The  $\zeta\zeta'^2$  and  $\zeta(\partial\zeta)^2$  shapes are correlated with the **local** template. In most cases there is a moderate overlap with the **enfolding** template. In some cases, corrections at subleading order (“next-order”) in the slow-roll expansion may become important. These have been catalogued in Ref. [36], to which we refer for details, for the action (2.2) with arbitrary  $\Lambda_i$ . These corrections therefore apply to an arbitrary action of Horndeski type.

**Bispectrum.** Factoring out an overall normalization, the shape  $S$  of the bispectrum can be written

$$S \propto \alpha S_{\zeta'^3} + \beta S_{\zeta\zeta'^2} + \gamma S_{\zeta(\partial\zeta)^2} + \delta S_{\zeta'\partial_i\zeta\partial^i(\partial^{-2}\zeta')} + \omega S_{\partial^2\zeta(\partial_i\partial^{-2}\zeta')^2}, \quad (2.5)$$

where  $\alpha, \beta, \gamma, \delta, \omega$  are rescaled versions of the coefficients  $\Lambda_i$ . In a generic model we could perhaps expect all these ratios to be order unity, although in specific cases some may be much smaller. By adjusting these coefficients it is possible to find a “critical surface” on which  $B$  becomes orthogonal to some specified set of templates. To be concrete, we choose the set  $Z = \{\text{equilateral, local, enfolding}\}$ . The bispectrum can be written

$$S \propto (\delta \ \omega) \begin{pmatrix} S_\delta \\ S_\omega \end{pmatrix} + (a \ b \ c) \begin{pmatrix} S_{\zeta'^3} \\ S_{\zeta\zeta'^2} \\ S_{\zeta(\partial\zeta)^2} \end{pmatrix}. \quad (2.6)$$

Here, the new shapes  $S_\delta$  and  $S_\omega$  are orthogonal by construction to each template in  $Z$ . The coefficients  $\delta$  and  $\omega$  act as coordinates on the subspace of bispectra which are also orthogonal to these templates. Likewise,  $a, b$  and  $c$  act as coordinates labelling departures from this critical subspace. They are defined by

$$\alpha \approx 2.394\delta + 2.208\omega + a \quad (2.7a)$$

$$\beta \approx 0.473\delta + 0.642\omega + b \quad (2.7b)$$

$$\gamma \approx -0.183\delta - 0.248\omega + c. \quad (2.7c)$$

The shapes  $S_\delta$  and  $S_\omega$  satisfy

$$S_\delta \approx 2.394S_{\zeta'^3} + 0.473S_{\zeta\zeta'^2} - 0.183S_{\zeta(\partial\zeta)^2} + S_{\zeta'\partial_i\zeta\partial^i(\partial^{-2}\zeta')} \quad (2.8a)$$

$$S_\omega \approx 2.208S_{\zeta'^3} + 0.642S_{\zeta\zeta'^2} - 0.248S_{\zeta(\partial\zeta)^2} + S_{\partial^2\zeta(\partial_i\partial^{-2}\zeta')^2}. \quad (2.8b)$$

Although we did not require it, these shapes are also highly orthogonal to the “orthogonal” template introduced by Senatore et al. [52]. (See also §3.) But they need not be orthogonal amongst themselves. To measure *independent* combinations from data typically

requires a dedicated template which has negligible overlap with other combinations. We follow the procedure of Refs. [9, 52]. The inner product matrix is  $C_{ij} \equiv S_i \cdot S_j$ . It is diagonalized by an orthogonal matrix  $\mathbf{P}$  whose columns are formed from the eigenvectors of  $\mathbf{C}$ . Setting  $a = b = c = 0$  and writing  $\mathbf{x} = (\delta \ \omega)$ ,  $\mathbf{S} = (S_\delta \ S_\omega)^\top$ , the part of bispectrum on the critical subspace can be written  $B^\parallel \propto \mathbf{q}\mathbf{H}$ , where  $\mathbf{q} \equiv \mathbf{x}\mathbf{P}$  and  $\mathbf{H} \equiv \mathbf{P}^\top \mathbf{S}$ .

The shapes  $S_{\zeta\zeta'^2}$  and  $S_{\zeta(\partial\zeta)^2}$  have local-type divergences, which can be subtracted by taking a suitable linear combination. This leaves four independent terms, from which we wish to construct a linear combination orthogonal to three templates. We should expect a unique solution. This can be extracted from  $\mathbf{H}$ , and is

$$S_H = -0.805S_\delta + 0.593S_\omega. \quad (2.9)$$

This procedure discards the independent linear combination of  $S_{\zeta\zeta'^2}$  and  $S_{\zeta(\partial\zeta)^2}$ . For practical purposes, we expect its divergence in the squeezed limit to make it almost indistinguishable from the local template. We ignore it in the equations which follow, such as (2.10), although in principle one should remember that it is present. In table 4 we plot  $S_H$  together with the ‘‘orthogonal’’ shapes which were encountered by Creminelli et al. [13] and Ref. [36].

These shapes are all similar. When plotted using the method of Babich et al. [8] the shape has a wavelike appearance. In the Fergusson et al. [51] plots of table 4, they smoothly converge to zero in the squeezed limit but exhibit distinctive ‘‘teardrop’’ or drumlin-shaped features near the corners of the triangle. The  $S_H$ -shape of Eq. (2.9) is closer to the shape of Creminelli et al. than the  $P(X, \phi)$ -based shape of Ref. [36]. However, the overall similarity suggests there is little difference in available shapes between different microphysical models. We will return to this issue in §3.

The shape  $S_H$  will occur in a typical bispectrum with coefficients which depend on  $\omega$  and  $\delta$ . We find

$$S = (0.593\omega - 0.805\delta)S_H + \begin{pmatrix} \alpha - 2.394\delta - 2.208\omega \\ \beta - 0.473\delta - 0.642\omega \\ \gamma + 0.183\delta + 0.248\omega \end{pmatrix} \begin{pmatrix} S_{\zeta'^3} \\ S_{\zeta\zeta'^2} \\ S_{\zeta(\partial\zeta)^2} \end{pmatrix}. \quad (2.10)$$

How significant is its contribution? Since all prefactors will generically be of order unity, the question reduces to the relative magnitudes of  $S_H$  and the  $S_a$ . We find  $\|S_H\| \approx 10^{-2}$ , whereas  $\|S_{\zeta'^3}\| \approx 1$ . The precise values assigned to  $\|S_{\zeta\zeta'^2}\|$  and  $\|S_{\zeta(\partial\zeta)^2}\|$  depend how their squeezed divergences are regulated, and therefore do not form a fair basis for comparison. Cutting out the divergent regions one finds  $\|S_{\zeta\zeta'^2}\|$  and  $\|S_{\zeta(\partial\zeta)^2}\|$  to be of order  $10^1$  to  $10^2$ . We conclude that  $S_H$  has an amplitude suppressed by roughly  $10^3$  to  $10^4$  compared with the leading-order shapes. All of these are well-matched by the standard templates. For the new shape  $S_H$  to be visible requires *either*

- The leading order shapes to be suppressed, so that  $a \approx b \approx c \approx 0$  to an accuracy of about a few parts in  $10^3$  to  $10^4$ . This could happen in a specific model, but requires some tuning.
- The overall amplitude of the bispectrum to be sufficiently large that the suppressed  $S_H$  shape is visible. Without a dedicated analysis of the signal-to-noise available in the  $S_H$ -channel for a CMB survey, it is not possible to know how large the bispectrum must be. However, it is unlikely that the signal to noise for  $S_H$  will be dramatically better than that for the `equilateral` template. Therefore, it seems reasonable to suggest that the leading-order operators would have to produce  $|f_{\text{NL}}^{\text{eq}}| \gtrsim 100$  in order for the  $S_H$ -shape to be visible. This is on the boundary of present-day experimental sensitivity [1, 52–54].

### 3 Partial-wave decomposition of the bispectrum

It is natural to ask why the various shapes obtained in §2.1 and Refs. [13, 36] are so similar. One answer is that they have all been constructed by taking linear combinations of similar-looking bispectra in a way designed to produce shapes orthogonal to the standard templates. Since the inputs are similar, so are the outputs.

Although this answer is correct, it does not make clear why a linear combination of dome-shaped bispectra should produce the characteristic drumlin shapes of table 4. The drumlin increases the number of nodes or anti-nodes exhibited by the bispectrum. One can think of its emergence in a similar way to taking two almost pure Fourier harmonics and constructing an orthogonal function. The result will be approximately the next available Fourier harmonic. Therefore, to obtain a more quantitative description one is led to decompose the bispectrum into some analogue of Fourier modes. The underlying triangular geometry is different to the flat intervals which yield Fourier harmonics, so the appropriate analogue will be a generalized partial wave.

**Harmonic decomposition.** Partial-wave decompositions have been usefully applied to correlation functions, in the form of scattering amplitudes, since the early days of quantum field theory. In  $WW$  scattering, partial-wave methods give guidance concerning the energy scale where the Standard Model without a Higgs boson loses perturbative unitarity. Similar ideas underlie, for example, the method of complex angular momenta and Regge theory. They have not been widely applied to inflationary correlation functions, although Fergusson et al. [37, 51] introduced a number of partial-wave decompositions and emphasized their computational efficiency. We largely follow their method and notation.<sup>2</sup>

---

<sup>2</sup>Physical conclusions must be independent of the basis, but the analysis may be made simpler by an appropriate choice. For comparison with the Fergusson et al. basis, we have repeated the analysis using Bessel functions [51]. With this choice, convergence is much slower. A different decomposition

Fergusson et al. suggested writing each shape function in the form

$$S(k_1, k_2, k_3) = \sum_n \alpha_n \mathcal{R}'_n(k_1, k_2, k_3), \quad (3.1)$$

for some coefficients  $\alpha_n$  and a set of dimensionless basis functions  $\mathcal{R}'_n$  which are orthonormal in the inner product (2.3).<sup>3</sup> The choice of  $\mathcal{R}'_n$  was motivated by numerical considerations, as follows. Define a complete set of orthonormal polynomials  $q_p(x)$  on the unit interval  $x \in [0, 1]$  with measure  $w(x)$  and introduce quantities  $\mathcal{Q}_{(p,q,r)}$  satisfying

$$\mathcal{Q}_{(p,q,r)} = q_p(2k_1/k_t)q_q(2k_2/k_t)q_r(2k_3/k_t) + 5 \text{ perms.} \quad (3.2)$$

Fergusson et al. chose  $w$  to cancel an unwanted growth in the bispectrum at large  $k$ ; for all details and the construction of the  $q_p(x)$  we refer to the original literature [37, 51]. One may impose a fixed normalization for the  $\mathcal{Q}_{(p,q,r)}$  if desired. They can be ordered by defining  $\rho^2 = p^2 + q^2 + r^2$  and sorting the  $\mathcal{Q}_{(p,q,r)}$  in ascending order of  $\rho$ . Finally, the  $\mathcal{R}'_n$  are constructed by Gram–Schmidt orthonormalization of the ordered  $\mathcal{Q}_{(p,q,r)}$ . It follows that the  $\mathcal{R}'_n$  are a linear combination of separable functions. This leads to efficiencies in computation of CMB observables, which was the principal motivation for Refs. [37, 51]. Because the  $\mathcal{R}'_n$  are orthonormal, one can obtain the expansion coefficients  $\alpha_n$  for any bispectrum  $B$  using the inner product (2.3),

$$\alpha_n = \langle \mathcal{R}'_n, B \rangle. \quad (3.3)$$

Note that  $\|B\|^2 = \sum_n \alpha_n^2$ , so one can interpret the ratio  $\alpha_n^2/\alpha_m^2$  as a measure of the relative importance of the  $m^{\text{th}}$  and  $n^{\text{th}}$  modes. We plot the first few  $\mathcal{R}'_n$  in Table 5 and quote  $\alpha_n$  for the common templates in Table 6. The  $n = 0$  mode is a constant. The  $n = 1, 2$  modes are a good match for the overall shape of both the **equilateral** and **orthogonal** templates. Strong features in the corners of the triangle, characteristic of the **local** shape, appear at higher  $n$ .

**Orthogonal combinations.** For our purposes, the usefulness of the  $\mathcal{R}'_n$  stems from the fact that the first three partial waves provide a very good description of the **equilateral**, **orthogonal** and **enfolded** templates. These can all be obtained by shifting the **equilateral** shape by a constant [9, 52]. The  $\mathcal{R}'_0$  shape is the constant shift. The “first

---

was used by Meerburg [55].

<sup>3</sup>The functions we are denoting  $\mathcal{R}'_n$  are only a subset of those constructed by Fergusson et al. [37, 51] and labelled  $\mathcal{R}_n$ . The  $\mathcal{R}'_n$  form a basis on a fixed slice at constant  $k_t = k_1 + k_2 + k_3$ . They are suitable for expansion of an approximately scale-invariant primordial bispectrum. The Fergusson et al.  $\mathcal{R}_n$  are not scale-invariant and are orthonormal in a three-dimensional inner product which accounts for variation in  $k_t$ . Our  $\mathcal{R}'_n$  are constructed using precisely the same procedure as the  $\mathcal{R}_n$ , but because many of the  $\mathcal{R}'_n$  are degenerate purely as a function of shape (but not scale) they are projected out of the  $\mathcal{R}'_n$ . It is in this sense that the  $\mathcal{R}'_n$  form a sparse subset of the  $\mathcal{R}_n$ .

harmonic,”  $\mathcal{R}'_1$ , peaks in the equilateral limit, whereas  $\mathcal{R}'_2$  peaks in the *flattened* configuration, where  $\alpha = \beta = 0$ . (This makes the two smallest  $k_i$  equal to one-half of the largest  $k_i$ .) These two peaks accurately describe the characteristics of the **equilateral/orthogonal/enfolded** class [52]. See also the discussion in Renaux-Petel et al. [17].

We quote expansion coefficients for the common templates in table 6, obtained using Eq. (3.3). For the reasons we have explained, the **equilateral, orthogonal and enfolded** templates are dominated by  $\{\mathcal{R}'_0, \mathcal{R}'_1, \mathcal{R}'_2\}$ , with their coefficients diminishing for higher  $n$ . This explains why the shape  $S_H$  of (2.9) has negligible overlap with the **orthogonal** template, even though this was not guaranteed by its construction. On the other hand, the **local** shape does not have a rapidly convergent expansion because its squeezed divergence requires a mixture of modes with  $n \gg 1$ . The net result is that the  $\mathcal{R}'_n$ -basis is reasonably well-adapted for an efficient description of the higher-derivative self-interactions of  $\zeta$ , which typically do not generate such divergences.

One can regard the orthogonalization process described in §2.1 as suppressing the coefficients of  $\{\mathcal{R}'_0, \mathcal{R}'_1, \mathcal{R}'_2\}$ . We give the expansion coefficients for the various “new” shapes in table 8. Consulting these coefficients shows that the  $\mathcal{R}'_0$  shape is projected out entirely for the shape of Creminelli et al. and the  $S_H$ -shape of (2.9). The situation for the  $P(X, \phi)$  shape is more complicated, and requires a separate discussion. For the remainder of this section we exclude it from our analysis. For the other two shapes, the  $n = 1, 2$  harmonics are not completely removed but their amplitudes are significantly reduced. As with the analogous case of Fourier harmonics, the largest individual term in each orthogonalized shape is a nearby higher mode—in this case, the  $n = 3$  term. (This is the next highest, although recall that the precise ordering of the  $\mathcal{R}'_n$  is somewhat arbitrary.) There is an admixture of the other harmonics with smaller amplitudes. Comparison with table 5 shows that the large  $n = 3$  contribution is essentially responsible for the common appearance of teardrops or drumlins. In practice, the broad hotspots of the  $\mathcal{R}'_3$  shape are slightly pinched by the presence of other harmonics at a lower level. In table 4, the right-hand columns give an approximation to each exact shape, formed from the first ten  $\mathcal{R}'_n$ . We quote the corresponding cosines in table 7. The approximations are extremely good, resulting in cosines in excess of 0.99.

The significance of this analysis is not that the  $S_H$ -shape can be roughly matched to an element of some complete, orthogonal basis of shapes. Such a basis always exists. Given a set of trial shapes, which could presumably be generated by considering arbitrarily exotic higher-derivative operators in the Lagrangian, this basis could be constructed precisely by the Gram–Schmidt procedure described in §2.1. It is more interesting that, at least for the low-dimension operators we are considering, the  $\mathcal{R}'_n$  basis provides an approximate match to the outcome of this process. Were we to continue adding new high-dimensional operators to the Lagrangian, the  $\mathcal{R}'_n$  shapes presumably give guidance about the shapes which could be expected to emerge from

the Gram–Schmidt procedure.

### 3.1 Distinguishing models

These properties imply that, instead of obtaining orthogonal combinations from the terms in the Lagrangian as in §2.1, it may be possible to do just as well with the  $\mathcal{R}'_n$  themselves.

Taken at face value, the common appearance of the shape in table 4 suggests that the *shape* of the bispectrum will not serve as a sensitive discriminant of microphysics. A significant **local** mode will favour dominantly local interactions, driven by gravitational evolution or the scalar potential, whereas a significant **equilateral** mode will favour strong, higher-derivative self-interactions. However, it seems difficult to be more precise. Instead of focusing on shapes, it may be more profitable to study relations between their *amplitudes* in order to distinguish among competing scenarios.

**Partial-wave amplitudes.** To proceed, we define a set of amplitudes  $\beta_n$  for an arbitrary bispectrum  $B$ ,

$$\langle B_{k_*}, \mathcal{R}'_n \rangle \equiv \beta_n \mathcal{P}^2(k_*), \quad (3.4)$$

where  $\mathcal{P}$  is the dimensionless power spectrum of the curvature perturbation. We will discuss the scale  $k_*$  below. The  $\beta_n$  are similar to the amplitudes  $f_{\text{NL}}^{\text{eq}}$ ,  $f_{\text{NL}}^{\text{orth}}$ , etc., which are used to place constraints on the nongaussian fraction observed in real data. Any predictive Lagrangian will depend on only a finite number of unknown parameters. If enough  $\beta_n$  can be estimated from data, then Eq. (3.4) allows these parameters to be expressed in terms of measurable quantities. The remaining relations in Eq. (3.4), when expressed in terms of these measurable quantities, constitute predictions of the theory. This is rather analogous to an on-shell renormalization scheme in scattering calculations by which one expresses “observables in terms of observables.” In inflation one usually speaks of “consistency equations” [56, 57].

In practice the precise  $\beta_n$  depend on the definition of the inner product, and indeed will vary between experiments. To perform a satisfactory analysis, one should obtain survey-dependent predictions for the  $\beta_n$ . The primordial bispectrum should be propagated to the surface of last scattering and projected on to the sky, and the  $\beta_n$  should be computed in the resulting two-dimensional inner product. The set of basis shapes should be orthogonal when measured using the experiment in question, and may not be directly related to the  $\mathcal{R}'_n$ . This will lead to numerically different  $\beta_n$  for each survey.

In what follows, we work for illustrative purposes with the primordial, three-dimensional bispectrum rather than the projected bispectrum. We make a number of simplifications. We use the inner product (2.3) in a scale-invariant approximation.<sup>4</sup> In evaluating  $\langle B, \mathcal{R}'_n \rangle$  one must choose a reference or ‘pivot’ scale at which to define  $B$ . We

---

<sup>4</sup>Our definition coincides with Ref. [36], in which a detailed discussion is given.

have denoted this scale  $k_*$ . The bispectrum then contains scale-dependent logarithms of the form  $\ln k/k_*$ , making  $\langle B, \mathcal{R}'_n \rangle$  a function of  $k_*$ . The power spectrum on the right-hand side of Eq. (3.4) is to be evaluated at  $k_*$ . Because our implementation of the inner product does not retain scale information, we cannot apply this prescription precisely. We replace such logarithms by  $\ln k/k_t$ , where  $k_t = k_1 + k_2 + k_3$  is the total scalar 3-momentum. This is likely to make an impact on our numerical coefficients at next-order, which should therefore be considered approximate.

**Example: DBI inflation.** As an illustration, we consider DBI inflation governed by the action

$$S = \int d^4x \sqrt{-g} \left( -\frac{1}{f(\phi)} \left[ \sqrt{1 - f(\phi)X} - 1 \right] - V(\phi) \right), \quad (3.5)$$

where  $X = -g^{ab}\partial_a\phi\partial_b\phi$ . This is a simple action in the Horndeski class. Based on a microscopic interpretation of (3.5) as the action for a brane of constant tension falling in a warped throat, the function  $f(\phi)$  is known as the warp factor. The potential is  $V(\phi)$ , and we define  $\gamma \equiv (1 - f\dot{\phi}^2)^{-1/2}$ . This action is known to lead to strong nongaussianities if  $\gamma \gtrsim 1$  [58, 59]. The inflationary fluctuations depend on the parameters [60]

$$\epsilon = \frac{1}{2} \left( \frac{V'}{V} \right)^2, \quad \eta = \frac{V''}{V}, \quad \text{and} \quad \Delta = \text{sgn}(\dot{\phi}f^{1/2}) \frac{f'}{f^{3/2}} \frac{1}{3H}, \quad (3.6)$$

where primed quantities are differentiated with respect to  $\phi$ . These must typically be small. The bispectrum was determined to  $\mathcal{O}(\epsilon, \eta, \Delta)$  in Ref. [36].<sup>5</sup>

The Lagrangian depends on the parameters of Eq. (3.6) and  $\gamma$ . We will therefore require *four* observables to fix these parameters. A *fifth* observable enables the theory to be tested. The presently well-measured parameters are only the amplitude,  $\mathcal{P}$ , and tilt,  $n_s$ , of the scalar power spectrum. There are relatively weak constraints on a

---

<sup>5</sup>To this accuracy one must typically retain gravitational interactions, which are often subdominant in models where the bispectrum has significant amplitude. Working in the uniform curvature slicing, a typical component of the metric is the perturbed lapse,  $\delta g_{00} \sim \varepsilon\zeta$ . At quadratic order this will enter via an operator such as  $(\partial\phi)^2$ . The leading quadratic operator without mixing is  $\sim M^2\dot{\zeta}^2$ , where  $M$  is the mass scale in (2.2). The leading mixing will be roughly  $\sim M^2\varepsilon H\zeta\dot{\zeta}$ . An overdot represents a time derivative, but for this power-counting exercise it could be replaced by a generic derivative. We estimate the contribution of each operator to a correlation function evaluated at characteristic energy scale  $E$  by setting  $\dot{\zeta} \sim E\zeta$ . This Minkowski estimate should be valid up to horizon exit, where we wish to estimate the relative importance of each operator to the density fluctuations which freeze in at that time. It follows that mixing with the metric can be neglected if  $E \gtrsim \varepsilon H$ .

In Ref. [11], subleading corrections were determined for the covariant Galileon action. However, this reference worked in the decoupling limit in which mixing with the metric was ignored. Typically this will not be consistent, so the *quantitative* magnitude of the next-order corrections in Ref. [11] should be treated only as a guide. In Ref. [36], whose results we rely on above, the mixing with the metric was retained.

few modes of the bispectrum. In the future it may be possible to detect the tensor amplitude  $\mathcal{P}_g$ . Assuming it will eventually be possible to measure  $\beta_0$  and  $\beta_1$  together with the tensor-to-scalar ratio,  $r \equiv \mathcal{P}_g/\mathcal{P}$ , then using the results of Ref. [36] and assuming at least moderate  $\gamma$  we find

$$\left(2.88\frac{\beta_1}{\beta_0} - 1\right) = 1.93(n_s - 1) + 0.03r\sqrt{-\beta_0} + 2.87\left(6.60\frac{\beta_2}{\beta_0} + 1\right). \quad (3.7)$$

Note that the DBI model predicts  $\beta_0 < 0$  if the bispectrum is large enough to be observable, as we will explain below. If  $r$  cannot be measured, or only with poor accuracy, then it will be necessary to use  $\beta_3$  as a substitute. In this case, we find

$$\left(2.88\frac{\beta_1}{\beta_0} - 1\right) = 0.65(n_s - 1) - 0.02\left(6.60\frac{\beta_2}{\beta_0} + 1\right) - 0.17\left(34.98\frac{\beta_3}{\beta_0} + 1\right). \quad (3.8)$$

In writing Eqs. (3.7)–(3.8) we must recall that observables (such as the  $\beta_n$ ) may mix Lagrangian *parameters* at lowest-order, next-order or other higher orders. The  $\beta_n$  begin at lowest-order, whereas  $n_s - 1$  and  $r$  begin at next-order. Therefore, in constructing (3.7)–(3.8) we have assumed

$$\left|2.88\frac{\beta_1}{\beta_0} - 1\right| \sim \left|6.60\frac{\beta_2}{\beta_0} + 1\right| \lesssim |n_s - 1| \sim r. \quad (3.9)$$

Whether Eq. (3.7) or (3.8) is more useful depends on the relative difficulty of measuring  $r$  and  $\beta_3$ . These expressions constitute a *model-independent* test of the DBI framework: they hold for any DBI action, up to  $\mathcal{O}(\epsilon, \eta, \Delta)$ , no matter what potential or warp factor is chosen. By showing they are not satisfied, one could rule out the DBI action as the origin of the inflationary perturbations. Of course, there is not a one-to-one mapping from models to consistency relations such as (3.7)–(3.8), and determining that any such equation *is* satisfied does not provide decisive evidence in favour of a model. The utility of such equations lies with their power to rule models out. However, showing that the  $\beta_n$  satisfy a hierarchy of consistency equations derived from some Lagrangian would be circumstantial evidence in favour of that model, especially if the agreement could be shown to persist to large  $n$ .

Eqs. (3.7)–(3.8) are analogues of the “next-order” consistency equations for the tensor tilt,  $n_t$  (cf. Eqs. (5.6)–(5.7) of Lidsey et al. [61]). If the  $\beta_n$  cannot be determined with sufficient accuracy to test these equations, we can obtain a simpler set of “lowest-order” relations obtained by systematically neglecting next-order terms, which entails  $n_s - 1 \approx r \approx 0$ . Together with (3.7)–(3.8), Eq. (3.9) then implies

$$2.88\frac{\beta_1}{\beta_0} \approx -6.60\frac{\beta_2}{\beta_0} \approx 1. \quad (3.10)$$

Even more simply, Eq. (3.10) requires  $\beta_0$  and  $\beta_1$  to have the same sign, and  $\beta_2$  to have the opposite sign. By consulting the individual expressions for the  $\beta_n$ , it follows

that  $\beta_0$  and  $\beta_1$  must be negative but  $\beta_2$  should be positive whenever  $\gamma$  is moderately large. This test is applicable even if the  $\beta_n$  cannot be determined accurately. In the present framework, it is a manifestation of the well-known result that the DBI model produces  $f_{\text{NL}}^{\text{eq}} < 0$ , whereas WMAP data favour  $f_{\text{NL}}^{\text{eq}} \gtrsim 0$ . For this reason, present-day observations are sufficient to disfavour DBI inflation. Note that Eq. (3.10), and similar expressions for  $\beta_n$  with  $n > 2$ , express the expected decrease in amplitude of  $\langle B, \mathcal{R}'_n \rangle$  with increasing  $n$ . The decrease is not monotonic, because the spikes which appear in  $\mathcal{R}'_n$  at larger  $n$  cause a small enhancement. However, the  $n = 0, 1, 2$  harmonics are larger than the rest, which is required by the analysis of §2.1.

**Example:  $k$ -inflation.** For comparison, consider the power-law  $k$ -inflation model of Armendáriz-Picón et al. [62]. The action for this model satisfies

$$S = \int d^4x \sqrt{-g} \frac{4}{9} \frac{4 - 3\gamma}{\gamma^2} \frac{X^2 - X}{\phi^2}. \quad (3.11)$$

It admits an inflationary solution for  $X = (2 - \gamma)/(4 - 3\gamma)$  provided  $0 < \gamma < 2/3$ . (Note that  $\gamma$  in this model is just a parameter, not related to the  $\gamma$  of the DBI model.) In the limit  $\gamma \ll 1$ , and keeping only leading-order terms, this model predicts

$$2.61 \frac{\beta_1}{\beta_0} = -4.80 \frac{\beta_2}{\beta_0} = 1. \quad (3.12)$$

Comparison with (3.10) shows that it would be necessary to measure  $\beta_0/\beta_1$  to about 10% in order to distinguish these models. A sufficiently accurate measurement of  $\beta_2$  would make the test considerably easier to apply.

This method is closely related to a trispectrum-based test for single-field inflation proposed by Smidt et al. [63]. The trispectrum contains contributions from two different ‘local’ shapes, with amplitudes parametrized by  $\tau_{\text{NL}}$  and  $g_{\text{NL}}$  [64–66]. The  $\tau_{\text{NL}}$  contribution obeys the Suyama–Yamaguchi inequality  $\tau_{\text{NL}} \geq (6f_{\text{NL}}^{\text{local}}/5)^2$  [67, 68]. Smidt et al. suggested studying  $A = \tau_{\text{NL}}/(6f_{\text{NL}}^{\text{local}}/5)^2$ , which is analogous to the ratios  $\beta_n/\beta_0$  introduced above. Their analysis suggested that Planck may be able to measure  $A$  to  $\pm 1.0$  at  $1\sigma$ , and a future CMB satellite may even be able to achieve  $\pm 0.3$  with the same significance. An accurate measurement of  $A > 1$  would be sufficient to rule out single-field scenarios.

Like the well-known standard inflationary consistency relation, whether relationships such as (3.7)–(3.10) and (3.12) are useful in practice will depend on the accuracy with which each component can be measured. This depends on the signal-to-noise associated with each shape. However, the method we have described can be implemented with *any* suitable basis; it is not restricted to the  $\mathcal{R}'_n$  functions described above.

## 4 Conclusions

Whichever microphysics operated in the very early Universe, its remnants are encoded in the CMB radiation. The imminent arrival of *Planck* data will enable us to assemble a detailed picture of the microwave sky, accompanied by important information concerning the statistics of the temperature and polarization fields. Searching for non-gaussianities in these statistics is a promising strategy to determine the details of interactions during the inflationary era.

In this paper, we have revisited the bispectrum in very general models of single-field inflation, which has recently been obtained by Gao & Steer [14] (see also Renaux-Petel [16]) and de Felice & Tsujikawa [15]. These computations demonstrated that, even in very general scenarios, the inflationary fluctuations would be generated by the same Lagrangian operators which are present in much simpler scenarios such as  $k$ -inflation. The difference lies only in the pattern of correlations among their coefficients, which varies between scenarios. We have shown that, although a potentially distinctive shape can be generated by these generalized models, it requires a degree of fine-tuning (or a large overall bispectrum). In any case, this shape is similar to one which has been encountered elsewhere [13, 36]. We conclude that it will be very difficult to distinguish between single-field models purely by detecting shapes in the bispectrum, although useful qualitative guidance could perhaps be obtained.

The natural alternative is to study correlations among the amplitudes of shapes which *are* present. For this purpose one may use templates or decompose the bispectrum into an orthogonal basis. For illustration, we use a basis proposed by Fergusson et al. [37, 51]. A given Lagrangian will typically generate fluctuations which depend on a finite number of parameters. If enough modes of the bispectrum can be determined with sufficient accuracy, these parameters can be written in terms of observable quantities. Further observations then constitute tests of any particular model.

As an illustration, we have applied our method to DBI inflation with an arbitrary potential and warp factor, and compared with the  $k$ -inflation scenario. With sufficiently accurate observations it may be possible to distinguish these scenarios. However, similar tests can be devised for any single-field inflationary model.

## Acknowledgments

We would like to thank Daniel Baumann, Clare Burrage, Anne Davis, James Fergusson, Eugene Lim, Donough Regan and Sébastien Renaux-Petel for helpful discussions. RHR is supported by Fundação para a Ciência e a Tecnologia through the grant SFRH/BD/35984/2007 and acknowledges the hospitality of the University of Sussex whilst this work was being completed. DS was supported by the Science and Technology Facilities Council [grant number ST/F002858/1].

## A Shape functions—different parametrizations

In plotting the bispectrum shapes we have used two parametrizations, which we describe in what follows.

**Babich et al.** This consists in factorizing one of the wavenumbers, say  $k_3$ , in the bispectrum amplitude, and rescale the independent remaining momenta accordingly, such that  $0 \leq k_1/k_3, k_2/k_3 \leq 1$ . The shape function is given by

$$\left(\frac{k_1}{k_3}\right)^2 \left(\frac{k_2}{k_3}\right)^2 B\left(\frac{k_1}{k_3}, \frac{k_2}{k_3}, 1\right).$$

**Fergusson & Shellard.** In this parametrization the privileged momentum scale is given by the semi-perimeter of the triangular configuration, used to define new variables  $\alpha$  and  $\beta$ , which satisfy

$$k_1 = \frac{k_t}{4}(1 + \alpha + \beta), \quad k_2 = \frac{k_t}{4}(1 - \alpha + \beta), \quad \text{and} \quad k_3 = \frac{k_t}{2}(1 - \beta).$$

The range of domain of  $\beta$  is  $0 \leq \beta \leq 1$ , whereas  $\beta - 1 \leq \alpha \leq 1 - \beta$ . The shape function is given by the combination

$$k_1^2 k_2^2 k_3^2 B(k_1, k_2, k_3).$$

Babich et al.

Fergusson & Shellard

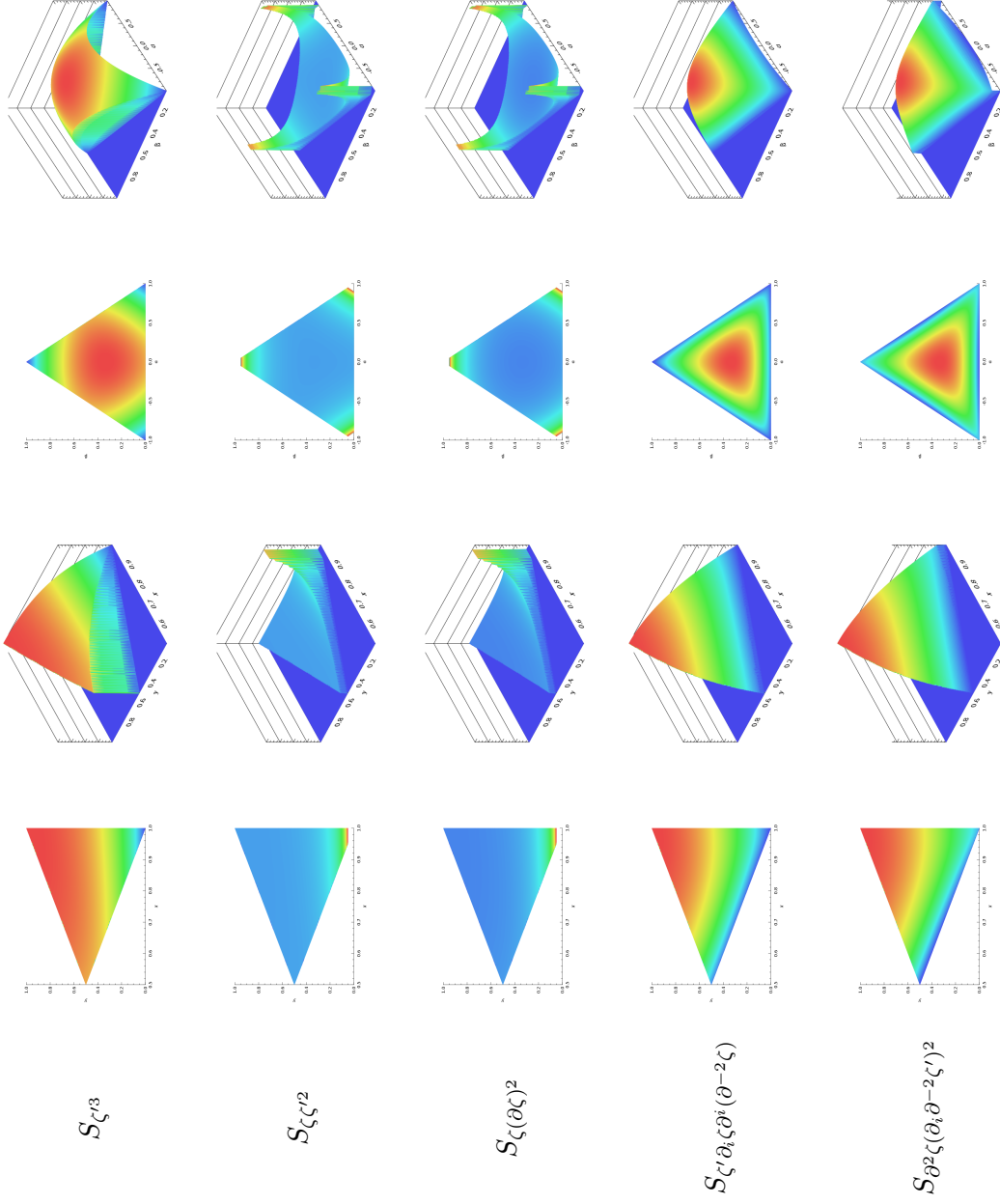


**Table 1.** Bispectrum shapes at leading order for the operators in the action (2.2), using the Babich et al. [8] and Fergusson-Shellard [51] parametrizations (see appendix).

shapes at leading order					
	$S_{\zeta'^3}$	$S_{\zeta\zeta'^2}$	$S_{\zeta(\partial\zeta)^2}$	$S_{\zeta'\partial_i\zeta\partial^i(\partial^{-2}\zeta')}$	$S_{\partial^2\zeta(\partial_i\partial^{-2}\zeta')^2}$
local	0.42	0.99	1.00	0.35	0.31
equilateral	0.94	0.44	0.38	1.00	0.99
orthogonal	0.29	0.50	0.49	0.02	0.12
enfolding	0.75	0.65	0.62	0.55	0.43

**Table 2.** Cosines between the leading order shapes and the common templates used in CMB analysis.

local <sup>a</sup>	equilateral	orthogonal	enfolding	Creminelli et al. <sup>b</sup>	$P(X, \phi)^c$
0.02	0.00	0.00	0.00	0.99	0.86

<sup>a</sup> The local template is divergent and requires choosing an appropriate regulator.

<sup>b</sup> This is the shape studied by Creminelli et al. [13].

<sup>c</sup> This is the shape  $\mathcal{O}$  constructed at next-order in  $P(X, \phi)$  models [36]. For the purpose of comparison, an appropriate normalization of the  $P(X, \phi)$  spectrum has been chosen.

**Table 3.** Cosines between the  $S_H$ -shape (2.9) and common templates.

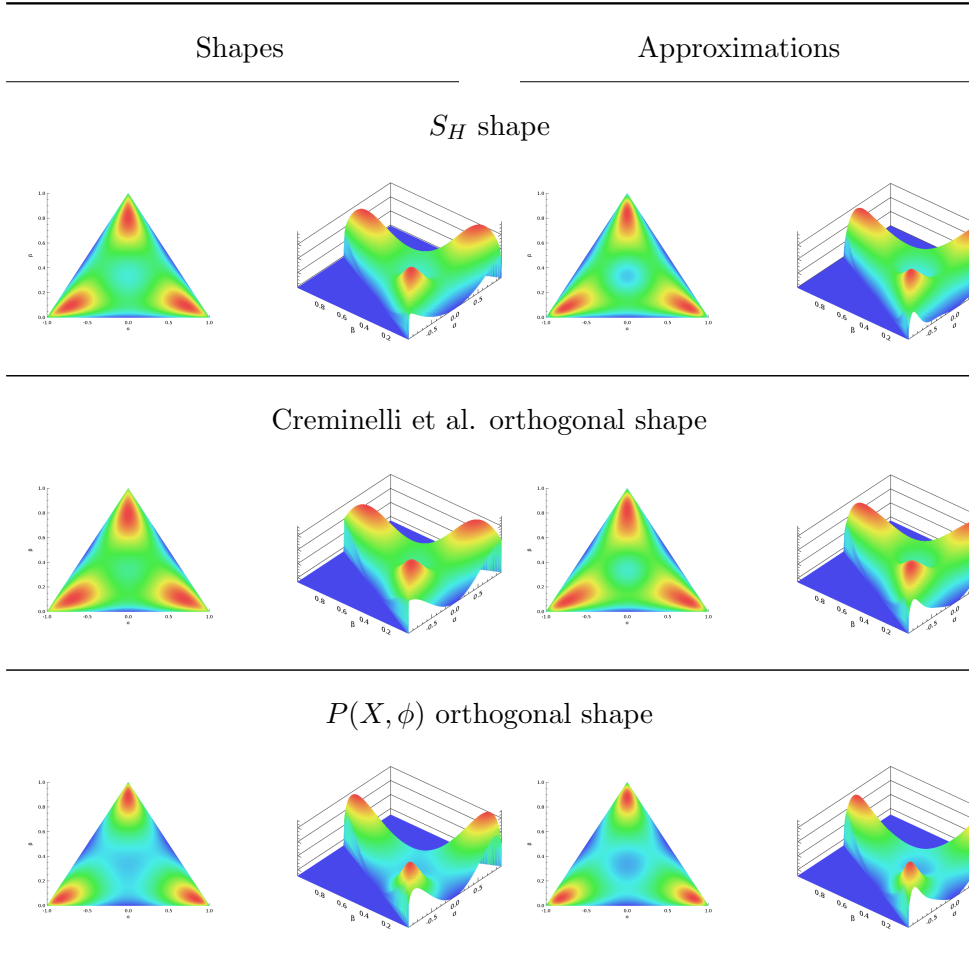


**Table 4.** Approximations to the  $S_H$ -shape and similar bispectra, up to the first ten harmonics in the  $\mathcal{R}_n$  expansion. The coefficients  $\alpha_n$  are listed in table 8.

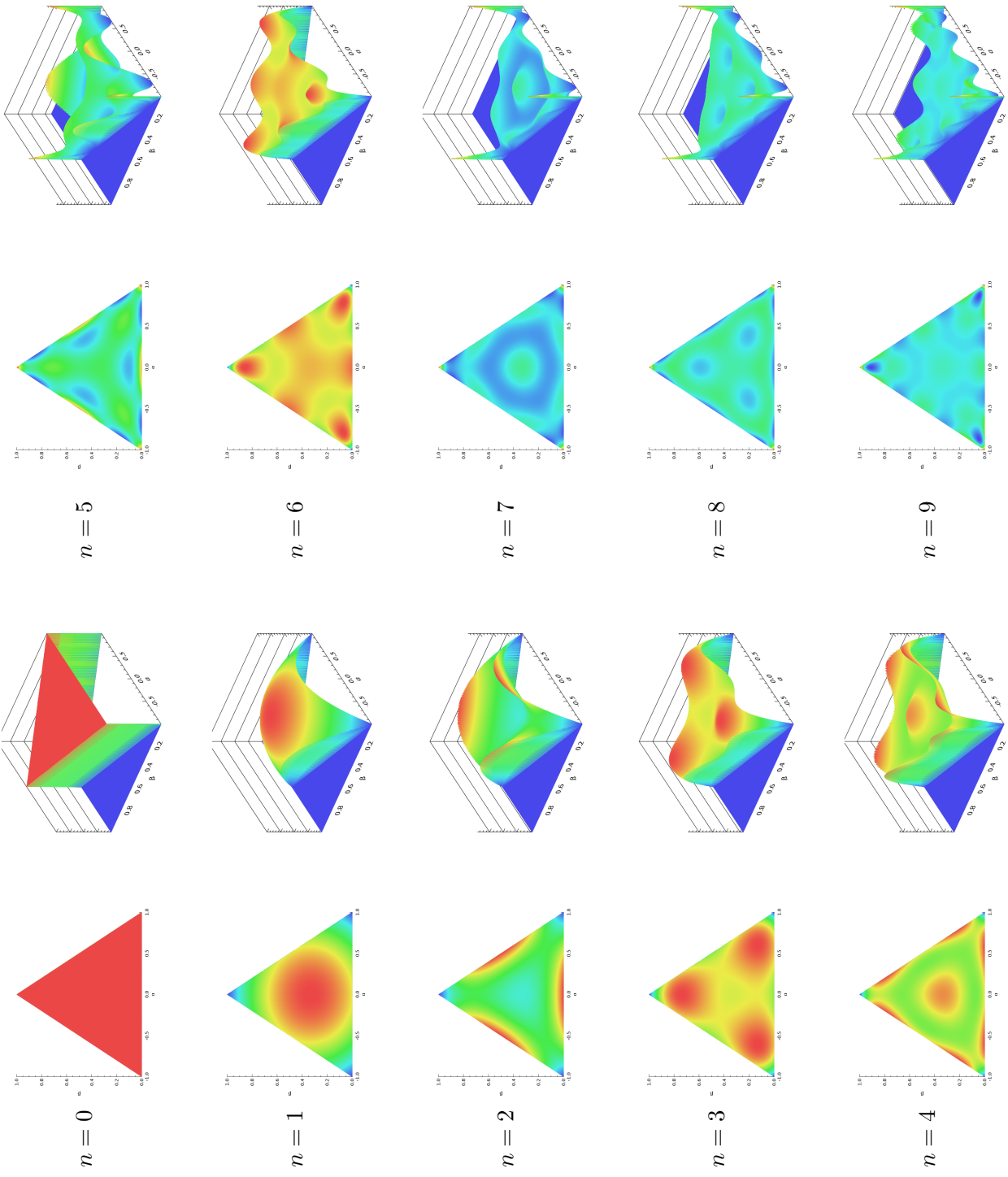


Table 5. Basis shapes  $\mathcal{R}'_n$ .

	$\alpha_0$	$\alpha_1$	$\alpha_2$	$\alpha_3$	$\alpha_4$	$\alpha_5$	$\alpha_6$	$\alpha_7$	$\alpha_8$	$\alpha_9$
local	-2.16	1.78	0.75	-1.21	0.79	-0.49	0.85	1.01	-0.53	-0.55
equilateral	0.52	0.23	-0.16	-0.03	-0.01	0.02	0.00	0.05	0.02	-0.01
orthogonal	-0.44	0.68	-0.49	-0.10	-0.04	0.07	0.01	0.13	0.05	-0.03
enfolding	0.48	-0.23	0.16	0.03	0.01	-0.02	0.00	-0.04	-0.02	0.01

**Table 6.** Expansion of common templates in terms of the  $\mathcal{R}'_n$  basis.

Approximations to orthogonal shapes			
	$S_H$ shape	Creminelli et al. shape <sup>a</sup>	$P(X, \phi)$ shape <sup>b</sup>
$S_H$ shape	0.99	0.98	0.89
Creminelli et al. shape <sup>a</sup>	0.97	0.99	0.88
$P(X, \phi)$ shape <sup>b</sup>	0.82	0.83	1.00

<sup>a</sup> This is the shape investigated by Creminelli et al. [13].

<sup>b</sup> This is the shape  $O$  constructed from contributions to the bispectrum at next-order in slow-roll [36].

**Table 7.** Cosines between  $\mathcal{R}'_n$ -approximations to the orthogonal shapes depicted in table 4 and the corresponding exact shape.

	$\alpha_0$	$\alpha_1$	$\alpha_2$	$\alpha_3$	$\alpha_4$	$\alpha_5$	$\alpha_6$	$\alpha_7$	$\alpha_8$	$\alpha_9$
$S_H$ -shape	0.000	0.006	0.006	0.010	0.005	-0.002	-0.002	-0.005	-0.003	0.002
$P(X, \phi)$ shape $O$	0.047	-0.190	-0.100	-0.107	-0.024	0.026	0.028	0.043	0.024	-0.019
Cremellini et al. shape	0.000	0.015	0.019	0.024	0.011	-0.006	-0.002	-0.012	-0.006	0.003

**Table 8.** Expansion of the  $S_H$ -shape, the  $P(X, \phi)$  shape  $O$  (at next-order) [36] and the Cremellini et al. shape [13] in terms of the  $\mathcal{R}'_n$  basis.

## References

- [1] **WMAP Collaboration** Collaboration, E. Komatsu *et al.*, *Seven-Year Wilkinson Microwave Anisotropy Probe (WMAP) Observations: Cosmological Interpretation*, *Astrophys.J.Suppl.* **192** (2011) 18, [[arXiv:1001.4538](#)], [[doi:10.1088/0067-0049/192/2/18](#)].
- [2] D. Larson, J. Dunkley, G. Hinshaw, E. Komatsu, M. Nolta, *et al.*, *Seven-Year Wilkinson Microwave Anisotropy Probe (WMAP) Observations: Power Spectra and WMAP-Derived Parameters*, *Astrophys.J.Suppl.* **192** (2011) 16, [[arXiv:1001.4635](#)], [[doi:10.1088/0067-0049/192/2/16](#)].
- [3] N. Jarosik, C. Bennett, J. Dunkley, B. Gold, M. Greason, *et al.*, *Seven-Year Wilkinson Microwave Anisotropy Probe (WMAP) Observations: Sky Maps, Systematic Errors, and Basic Results*, *Astrophys.J.Suppl.* **192** (2011) 14, [[arXiv:1001.4744](#)], [[doi:10.1088/0067-0049/192/2/14](#)].
- [4] A. H. Guth, *The Inflationary Universe: A Possible Solution to the Horizon and Flatness Problems*, *Phys.Rev.* **D23** (1981) 347–356, [[doi:10.1103/PhysRevD.23.347](#)].
- [5] A. H. Guth and D. I. Kaiser, *Inflationary cosmology: Exploring the Universe from the smallest to the largest scales*, *Science* **307** (2005) 884–890, [[arXiv:astro-ph/0502328](#)], [[doi:10.1126/science.1107483](#)].
- [6] J. M. Bardeen, P. J. Steinhardt, and M. S. Turner, *Spontaneous Creation of Almost Scale - Free Density Perturbations in an Inflationary Universe*, *Phys.Rev.* **D28** (1983) 679, [[doi:10.1103/PhysRevD.28.679](#)].
- [7] E. Komatsu, N. Afshordi, N. Bartolo, D. Baumann, J. Bond, *et al.*, *Non-Gaussianity as a Probe of the Physics of the Primordial Universe and the Astrophysics of the Low Redshift Universe*, [arXiv:0902.4759](#).
- [8] D. Babich, P. Creminelli, and M. Zaldarriaga, *The shape of non-Gaussianities*, *JCAP* **0408** (2004) 009, [[arXiv:astro-ph/0405356](#)], [[doi:10.1088/1475-7516/2004/08/009](#)].
- [9] X. Chen, *Primordial Non-Gaussianities from Inflation Models*, *Adv.Astron.* **2010** (2010) 638979, [[arXiv:1002.1416](#)], [[doi:10.1155/2010/638979](#)].
- [10] K. Koyama, *Non-Gaussianity of quantum fields during inflation*, *Class.Quant.Grav.* **27** (2010) 124001, [[arXiv:1002.0600](#)], [[doi:10.1088/0264-9381/27/12/124001](#)].
- [11] C. Burrage, C. de Rham, D. Seery, and A. J. Tolley, *Galileon inflation*, *JCAP* **1101** (2011) 014, [[arXiv:1009.2497](#)], [[doi:10.1088/1475-7516/2011/01/014](#)].
- [12] D. Baumann and D. Green, *Equilateral Non-Gaussianity and New Physics on the Horizon*, *JCAP* **1109** (2011) 014, [[arXiv:1102.5343](#)], [[doi:10.1088/1475-7516/2011/09/014](#)]. \* Temporary entry \*.
- [13] P. Creminelli, G. D’Amico, M. Musso, J. Norena, and E. Trincherini, *Galilean symmetry in the effective theory of inflation: new shapes of non-Gaussianity*, *JCAP* **1102** (2011) 006, [[arXiv:1011.3004](#)], [[doi:10.1088/1475-7516/2011/02/006](#)].

- [14] X. Gao and D. A. Steer, *Inflation and primordial non-Gaussianities of “generalized Galileons”*, [arXiv:1107.2642](#).
- [15] A. De Felice and S. Tsujikawa, *Inflationary non-Gaussianities in the most general second-order scalar-tensor theories*, [arXiv:1107.3917](#).
- [16] S. Renaux-Petel, *On the redundancy of operators and the bispectrum in the most general second-order scalar-tensor theory*, [arXiv:1107.5020](#).
- [17] S. Renaux-Petel, S. Mizuno, and K. Koyama, *Primordial fluctuations and non-Gaussianities from multifield DBI Galileon inflation*, [arXiv:1108.0305](#).
- [18] S. E. Vazquez, *Constraining Modified Gravity with Large non-Gaussianities*, *Phys.Rev.* **D79** (2009) 043520, [[arXiv:0806.0603](#)], [[doi:10.1103/PhysRevD.79.043520](#)].
- [19] X. Gao, *Testing gravity with non-Gaussianity*, *Phys.Lett.* **B702** (2011) 197–200, [[arXiv:1008.2123](#)], [[doi:10.1016/j.physletb.2011.07.022](#)].
- [20] C. de Rham and G. Gabadadze, *Generalization of the Fierz-Pauli Action*, *Phys.Rev.* **D82** (2010) 044020, [[arXiv:1007.0443](#)], [[doi:10.1103/PhysRevD.82.044020](#)].
- [21] C. de Rham, G. Gabadadze, and A. J. Tolley, *Resummation of Massive Gravity*, *Phys.Rev.Lett.* **106** (2011) 231101, [[arXiv:1011.1232](#)], [[doi:10.1103/PhysRevLett.106.231101](#)].
- [22] S. Hassan and R. A. Rosen, *Resolving the Ghost Problem in non-Linear Massive Gravity*, [arXiv:1106.3344](#).
- [23] K. Hinterbichler, *Theoretical Aspects of Massive Gravity*, [arXiv:1105.3735](#).
- [24] G. Dvali, G. Gabadadze, and M. Porrati, *4-D gravity on a brane in 5-D Minkowski space*, *Phys.Lett.* **B485** (2000) 208–214, [[arXiv:hep-th/0005016](#)], [[doi:10.1016/S0370-2693\(00\)00669-9](#)].
- [25] C. Deffayet, G. Dvali, and G. Gabadadze, *Accelerated universe from gravity leaking to extra dimensions*, *Phys.Rev.* **D65** (2002) 044023, [[arXiv:astro-ph/0105068](#)], [[doi:10.1103/PhysRevD.65.044023](#)].
- [26] T. Kobayashi, M. Yamaguchi, and J. Yokoyama, *G-inflation: Inflation driven by the Galileon field*, *Phys.Rev.Lett.* **105** (2010) 231302, [[arXiv:1008.0603](#)], [[doi:10.1103/PhysRevLett.105.231302](#)].
- [27] S. Mizuno and K. Koyama, *Primordial non-Gaussianity from the DBI Galileons*, *Phys.Rev.* **D82** (2010) 103518, [[arXiv:1009.0677](#)], [[doi:10.1103/PhysRevD.82.103518](#)].
- [28] T. Kobayashi, M. Yamaguchi, and J. Yokoyama, *Primordial non-Gaussianity from G-inflation*, *Phys.Rev.D* (2011) [[arXiv:1103.1740](#)].
- [29] S. Renaux-Petel, *Orthogonal non-Gaussianities from Dirac-Born-Infeld Galileon inflation*, *Class.Quant.Grav.* **28** (2011) 182001, [[arXiv:1105.6366](#)], [[doi:10.1088/0264-9381/28/18/182001](#)]. \* Temporary entry \*.
- [30] T. Kobayashi, M. Yamaguchi, and J. Yokoyama, *Generalized G-inflation: Inflation*

with the most general second-order field equations, [arXiv:1105.5723](#).

- [31] G. W. Horndeski *Int. J. Theor. Phys.* **10** (1974) 363.
- [32] C. Charmousis, E. J. Copeland, A. Padilla, and P. M. Saffin, *General second order scalar-tensor theory, self tuning, and the Fab Four*, [arXiv:1106.2000](#).
- [33] C. Deffayet, S. Deser, and G. Esposito-Farese, *Generalized Galileons: All scalar models whose curved background extensions maintain second-order field equations and stress-tensors*, *Phys.Rev.* **D80** (2009) 064015, [[arXiv:0906.1967](#)], [[doi:10.1103/PhysRevD.80.064015](#)].
- [34] C. Deffayet, X. Gao, D. A. Steer, and G. Zahariade, *From k-essence to generalised Galileons*, [arXiv:1103.3260](#).
- [35] C. Cheung, P. Creminelli, A. Fitzpatrick, J. Kaplan, and L. Senatore, *The Effective Field Theory of Inflation*, *JHEP* **0803** (2008) 014, [[arXiv:0709.0293](#)], [[doi:10.1088/1126-6708/2008/03/014](#)].
- [36] C. Burrage, R. H. Ribeiro, and D. Seery, *Large slow-roll corrections to the bispectrum of noncanonical inflation*, *JCAP* **1107** (2011) 032, [[arXiv:1103.4126](#)], [[doi:10.1088/1475-7516/2011/07/032](#)]. \* Temporary entry \*.
- [37] J. Fergusson, M. Liguori, and E. Shellard, *General CMB and Primordial Bispectrum Estimation I: Mode Expansion, Map-Making and Measures of  $f_{\text{NL}}$* , *Phys.Rev.* **D82** (2010) 023502, [[arXiv:0912.5516](#)], [[doi:10.1103/PhysRevD.82.023502](#)].
- [38] A. Nicolis, R. Rattazzi, and E. Trincherini, *The Galileon as a local modification of gravity*, *Phys.Rev.* **D79** (2009) 064036, [[arXiv:0811.2197](#)], [[doi:10.1103/PhysRevD.79.064036](#)].
- [39] C. de Rham and A. J. Tolley, *DBI and the Galileon reunited*, *JCAP* **1005** (2010) 015, [[arXiv:1003.5917](#)], [[doi:10.1088/1475-7516/2010/05/015](#)].
- [40] C. Deffayet, G. Esposito-Farese, and A. Vikman, *Covariant Galileon*, *Phys.Rev.* **D79** (2009) 084003, [[arXiv:0901.1314](#)], [[doi:10.1103/PhysRevD.79.084003](#)].
- [41] G. Goon, K. Hinterbichler, and M. Trodden, *Symmetries for Galileons and DBI scalars on curved space*, *JCAP* **1107** (2011) 017, [[arXiv:1103.5745](#)], [[doi:10.1088/1475-7516/2011/07/017](#)].
- [42] G. Goon, K. Hinterbichler, and M. Trodden, *A New Class of Effective Field Theories from Embedded Branes*, *Phys.Rev.Lett.* **106** (2011) 231102, [[arXiv:1103.6029](#)], [[doi:10.1103/PhysRevLett.106.231102](#)].
- [43] M. Trodden and K. Hinterbichler, *Generalizing Galileons*, *Class.Quant.Grav.* **28** (2011) 204003, [[arXiv:1104.2088](#)], [[doi:10.1088/0264-9381/28/20/204003](#)].
- [44] C. Burrage, C. de Rham, and L. Heisenberg, *de Sitter Galileon*, *JCAP* **1105** (2011) 025, [[arXiv:1104.0155](#)], [[doi:10.1088/1475-7516/2011/05/025](#)].
- [45] A. Vainshtein, *To the problem of nonvanishing gravitation mass*, *Phys.Lett.* **B39** (1972) 393–394, [[doi:10.1016/0370-2693\(72\)90147-5](#)].

- [46] C. Burrage and D. Seery, *Revisiting fifth forces in the Galileon model*, *JCAP* **1008** (2010) 011, [[arXiv:1005.1927](#)], [[doi:10.1088/1475-7516/2010/08/011](#)].
- [47] R. Gannouji and M. Sami, *Galileon gravity and its relevance to late time cosmic acceleration*, *Phys. Rev.* **D82** (2010) 024011, [[arXiv:1004.2808](#)], [[doi:10.1103/PhysRevD.82.024011](#)].
- [48] A. Ali, R. Gannouji, and M. Sami, *Modified gravity a la Galileon: Late time cosmic acceleration and observational constraints*, *Phys.Rev.* **D82** (2010) 103015, [[arXiv:1008.1588](#)], [[doi:10.1103/PhysRevD.82.103015](#)].
- [49] P. Brax, C. Burrage, and A.-C. Davis, *Laboratory Tests of the Galileon*, *JCAP* **1109** (2011) 020, [[arXiv:1106.1573](#)], [[doi:10.1088/1475-7516/2011/09/020](#)].
- [50] C. Deffayet, O. Pujolas, I. Sawicki, and A. Vikman, *Imperfect Dark Energy from Kinetic Gravity Braiding*, *JCAP* **1010** (2010) 026, [[arXiv:1008.0048](#)], [[doi:10.1088/1475-7516/2010/10/026](#)].
- [51] J. R. Fergusson and E. P. S. Shellard, *The shape of primordial non-Gaussianity and the CMB bispectrum*, *Phys. Rev.* **D80** (2009) 043510, [[arXiv:0812.3413](#)], [[doi:10.1103/PhysRevD.80.043510](#)].
- [52] L. Senatore, K. M. Smith, and M. Zaldarriaga, *Non-Gaussianities in Single Field Inflation and their Optimal Limits from the WMAP 5-year Data*, *JCAP* **1001** (2010) 028, [[arXiv:0905.3746](#)], [[doi:10.1088/1475-7516/2010/01/028](#)].
- [53] P. Creminelli, A. Nicolis, L. Senatore, M. Tegmark, and M. Zaldarriaga, *Limits on non-gaussianities from WMAP data*, *JCAP* **0605** (2006) 004, [[arXiv:astro-ph/0509029](#)], [[doi:10.1088/1475-7516/2006/05/004](#)].
- [54] P. Creminelli, L. Senatore, M. Zaldarriaga, and M. Tegmark, *Limits on  $f_{\text{NL}}$  parameters from WMAP 3yr data*, *JCAP* **0703** (2007) 005, [[arXiv:astro-ph/0610600](#)], [[doi:10.1088/1475-7516/2007/03/005](#)].
- [55] P. Meerburg, *Oscillations in the Primordial Bispectrum I: Mode Expansion*, *Phys.Rev.* **D82** (2010) 063517, [[arXiv:1006.2771](#)], [[doi:10.1103/PhysRevD.82.063517](#)].
- [56] E. J. Copeland, E. W. Kolb, A. R. Liddle, and J. E. Lidsey, *Reconstructing the inflation potential, in principle and in practice*, *Phys.Rev.* **D48** (1993) 2529–2547, [[arXiv:hep-ph/9303288](#)], [[doi:10.1103/PhysRevD.48.2529](#)].
- [57] E. J. Copeland, E. W. Kolb, A. R. Liddle, and J. E. Lidsey, *Reconstructing the inflaton potential: Perturbative reconstruction to second order*, *Phys.Rev.* **D49** (1994) 1840–1844, [[arXiv:astro-ph/9308044](#)], [[doi:10.1103/PhysRevD.49.1840](#)].
- [58] M. Alishahiha, E. Silverstein, and D. Tong, *DBI in the sky*, *Phys. Rev.* **D70** (2004) 123505, [[arXiv:hep-th/0404084](#)], [[doi:10.1103/PhysRevD.70.123505](#)].
- [59] X. Chen, M.-x. Huang, S. Kachru, and G. Shiu, *Observational signatures and non-Gaussianities of general single field inflation*, *JCAP* **0701** (2007) 002, [[arXiv:hep-th/0605045](#)], [[doi:10.1088/1475-7516/2007/01/002](#)].

- [60] P. Franche, R. Gwyn, B. Underwood, and A. Wissanji, *Attractive Lagrangians for Non-Canonical Inflation*, *Phys.Rev.* **D81** (2010) 123526, [[arXiv:0912.1857](#)], [[doi:10.1103/PhysRevD.81.123526](#)].
- [61] J. E. Lidsey, A. R. Liddle, E. W. Kolb, E. J. Copeland, T. Barreiro, *et al.*, *Reconstructing the inflation potential : An overview*, *Rev.Mod.Phys.* **69** (1997) 373–410, [[arXiv:astro-ph/9508078](#)], [[doi:10.1103/RevModPhys.69.373](#)].
- [62] C. Armendariz-Picon, T. Damour, and V. F. Mukhanov, *k-inflation*, *Phys.Lett.* **B458** (1999) 209–218, [[arXiv:hep-th/9904075](#)], [[doi:10.1016/S0370-2693\(99\)00603-6](#)].
- [63] J. Smidt, A. Amblard, C. T. Byrnes, A. Cooray, A. Heavens, *et al.*, *CMB Constraints on Primordial non-Gaussianity from the Bispectrum ( $f_{\text{NL}}$ ) and Trispectrum ( $g_{\text{NL}}$  and  $\tau_{\text{NL}}$ ) and a New Consistency Test of Single-Field Inflation*, *Phys.Rev.* **D81** (2010) 123007, [[arXiv:1004.1409](#)], [[doi:10.1103/PhysRevD.81.123007](#)].
- [64] M. Sasaki, J. Valiviita, and D. Wands, *Non-Gaussianity of the primordial perturbation in the curvaton model*, *Phys.Rev.* **D74** (2006) 103003, [[arXiv:astro-ph/0607627](#)], [[doi:10.1103/PhysRevD.74.103003](#)].
- [65] C. T. Byrnes, M. Sasaki, and D. Wands, *The primordial trispectrum from inflation*, *Phys.Rev.* **D74** (2006) 123519, [[arXiv:astro-ph/0611075](#)], [[doi:10.1103/PhysRevD.74.123519](#)].
- [66] D. Seery and J. E. Lidsey, *Non-Gaussianity from the inflationary trispectrum*, *JCAP* **0701** (2007) 008, [[arXiv:astro-ph/0611034](#)], [[doi:10.1088/1475-7516/2007/01/008](#)].
- [67] T. Suyama and M. Yamaguchi, *Non-Gaussianity in the modulated reheating scenario*, *PHRVA,D77,023505.2008* **D77** (2008) 023505, [[arXiv:0709.2545](#)], [[doi:10.1103/PhysRevD.77.023505](#)].
- [68] K. M. Smith, M. LoVerde, and M. Zaldarriaga, *A universal bound on N-point correlations from inflation*, [arXiv:1108.1805](#).